

# Pulse Detonation Generated by Natural Gas Recirculation in Shale Gas Recovery

Z. Al-Dulaimi\*, Agustin Valera-Medina, Nick Syred, Richard Marsh, Phil Bowen  
*College of Physical Sciences and Engineering, Cardiff University*

## Abstract

Shale gas presents an opportunity to alleviate European dependence on imported gas, which is required for load matching within future renewable energy systems. However, shale gas has acquired a negative public image primarily due to ‘hydraulic fracturing’ extraction methods, commonly known as ‘fracking’, whose risks include air and water pollution. Hence, there is the need to appraise alternative proposals for shale gas extraction where environmental risks are mitigated or negated.

Producing high-pressure waves at the base of the wellbore by using small, control gaseous detonations offers promising potential for shale gas extraction, negating the primary risks associated with hydraulic fracturing. A fundamental study of deflagration to detonation transition using recirculated shale gas mixed with pure oxygen as an oxidiser has been undertaken within a programme to design a system with lower DDT distance and higher amplitude pressure waves. Three UK shale gas compositions were studied. The chemical equilibrium software GASEQ and chemical kinetic software CHEMKIN-PRO were used for simulation. Results show that the influence of diluents, such as carbon dioxide can be eliminated by the use of higher hydrogen-content species for the three cases proposed. OpenFOAM CFD was used to estimate the detonation-to-deflagration transition parameters in stoichiometric hydrogen/air mixtures to evaluate different obstacle geometries on the transition phenomenon. It was found that rectangular shape obstacles reduce the reaction time and hence decrease the run-up distance to achieve DDT whilst, semi-circular shaped obstacles generate the highest pressure in a detonation tube. The outcome from numerical predictions is guiding the construction of an experimental programme with different obstacle configurations to demonstrate the concept of consistent pulse detonation for shale-rock cracking.

## Introduction

Increase in shale gas production has decreased both natural gas wholesale prices and dependence on imports. However, the main concern of shale gas extracting is its environmental risks. Hydraulic fracturing has been used for hydrocarbon well stimulation since the mid-twentieth century. This technology has become the main trend for exploitation of shale gas [1, 2].

There are several technologies for fracturing, amongst which hydraulic fracturing, pneumatic fracturing and dynamic-loading fracturing are the most prevalent [2-5].

Producing repeated high-pressure waves at the base of the well bore using gaseous detonations presents a potential alternative technique for shale gas extraction. This technique has the potential to overcome both small distance fracturing with dynamic loading and the environmental disadvantages of hydraulic fracking. Detonation waves are essentially shock waves with energy evolution within the wave front. The interaction of pressure waves travelling ahead of the flame with the boundary layer formed by the precursor shock is an important contributory factor to trigger the detonation. The crucial role is played by thermodynamic interactions and the induction time.

When reactants are ignited, a combustion wave is generated which propagates away from the ignition source. Physical and chemical processes, which are generated by the gradient fields across the wave, lead the combustion wave becoming self-sustained.

During the initial stage of flame propagation, just after ignition, the main source of the flame acceleration is the increasing surface area of the flame [6]. When the flame hits the back and side walls of the confinement pipe, the flame propagation passes through four stages Figure 1 shows these well established processes, which are described in detail elsewhere [7].

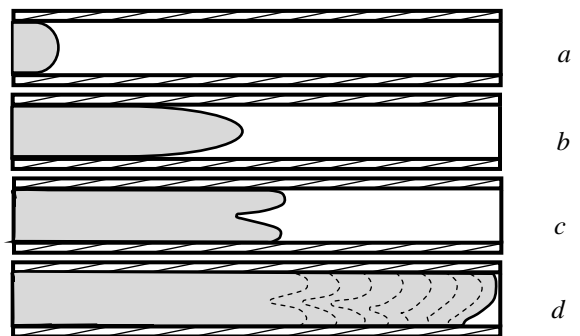


Figure 1. The four stages of flame propagation in confined geometry.

- a. Hemispherical shape.    b. Finger shaped.  
c. Tulip flame.            d. Flame surface inversion.

Deflagration waves are inherently unstable. Under certain conditions pertaining primarily to fuel and geometrical characteristics, the flame speed can continuously accelerate to reach conditions conducive to the spontaneous onset of detonation [8]. The distance required for deflagration to detonation (predetonation distance) is also influenced by many factors. For instance, the presence of obstacles in pipes containing propagating flames leads to increased turbulence, which in turn, increases the

-----  
\* Corresponding author: [Al-DulaimiZM@cardiff.ac.uk](mailto:Al-DulaimiZM@cardiff.ac.uk)  
Proceedings of the European Combustion Meeting 2017

local burning rate by increasing both the surface area of the flame and, depending upon fuel type, the transport of local mass and energy. This leads to higher flow velocity in the unburned gas and increased pressure. All of these actions, under appropriate conditions, can contribute to the inception of detonation [9].

This project analyses different configurations giving rise to deflagration to detonation transitions using typical shale gas compositions. The program has been based on the use of numerical codes to explore design options that will inform and be validated in a subsequent experimental programme.

## Methodology

### Case Selection

Stamford and Azapagic [10] proposed three cases for shale gas composition, namely best case, central case and worst case, depending on the parameters they considered in their study, Table 1. Methane concentration ranged between 73% to 55%, with a variety of other species in each case. These three shale gas compositions were used with pure oxygen as an oxidiser to calculate the product properties when detonated utilising GASEQ and CHEMKIN-PRO software for chemical analysis. OpenFOAM is used in the present work to include the flow fields generated by different internal geometries and their influence on flame propagation leading to transition conditions.

Table 1: Shale gas composition as suggested by Stamford et al. [10].

High Case	Central Case	Low Case
<ul style="list-style-type: none"> <li>• CH<sub>4</sub> 0.61kg/m<sup>3</sup></li> <li>• C<sub>2</sub>H<sub>6</sub> 0.04kg/m<sup>3</sup></li> <li>• C<sub>4</sub>H<sub>10</sub> 0.04kg/m<sup>3</sup></li> <li>• Other alkanes 0.02kg/m<sup>3</sup></li> <li>• CO<sub>2</sub> 0.13kg/m<sup>3</sup></li> <li>• He 0.001kg/m<sup>3</sup></li> <li>• Hg 2×10<sup>-7</sup>kg/m<sup>3</sup></li> <li>• Rn 400Bq/m<sup>3</sup></li> </ul>	<ul style="list-style-type: none"> <li>• CH<sub>4</sub> 0.555kg/m<sup>3</sup></li> <li>• C<sub>2</sub>H<sub>6</sub> 0.075kg/m<sup>3</sup></li> <li>• C<sub>3</sub>H<sub>8</sub> 0.05kg/m<sup>3</sup></li> <li>• C<sub>4</sub>H<sub>10</sub> 0.02kg/m<sup>3</sup></li> <li>• Other alkanes 0.03kg/m<sup>3</sup></li> <li>• CO<sub>2</sub> 0.115kg/m<sup>3</sup></li> <li>• H<sub>2</sub>S 0.045kg/m<sup>3</sup></li> <li>• N<sub>2</sub> 0.03kg/m<sup>3</sup></li> <li>• He 0.001kg/m<sup>3</sup></li> <li>• Hg 2×10<sup>-7</sup>kg/m<sup>3</sup></li> <li>• Rn 400Bq/m<sup>3</sup></li> </ul>	<ul style="list-style-type: none"> <li>• CH<sub>4</sub> 0.5kg/m<sup>3</sup></li> <li>• C<sub>2</sub>H<sub>6</sub> 0.11kg/m<sup>3</sup></li> <li>• C<sub>3</sub>H<sub>8</sub> 0.105kg/m<sup>3</sup></li> <li>• Other alkanes 0.04kg/m<sup>3</sup></li> <li>• CO<sub>2</sub> 0.1kg/m<sup>3</sup></li> <li>• H<sub>2</sub>S 0.09kg/m<sup>3</sup></li> <li>• N<sub>2</sub> 0.03kg/m<sup>3</sup></li> <li>• He 0.001kg/m<sup>3</sup></li> <li>• Hg 2×10<sup>-7</sup>kg/m<sup>3</sup></li> <li>• Rn 400Bq/m<sup>3</sup></li> </ul>

### 0-D and 1-D Analysis

GASEQ, a 0-D analysis software, is a Microsoft Windows programme which calculates chemical equilibrium for combustion. The combustion calculations are made on the basis of thermodynamic equilibrium and minimisation of free energy [11]. CHEMKIN-PRO software was also utilised for 1-D analysis. CHEMKIN is one of the most popular codes for simulating chemical reaction and analysing chemical kinetics [12-13].

The Gas Research Institute mechanism, GRI-Mech 3.0, was chosen for this study as it is designed to model natural gas and methane combustion. Although this mechanism is considered as one of the

most popular single carbon reaction mechanism, it also includes other fuel combustion mechanism, such as the detailed combustion reaction mechanism for hydrogen [14]. The detailed GRI-Mech 3.0 mechanism consists of 325 reaction steps and 53 species with associated rate coefficient expressions and thermochemical parameters.

### 2-D Analysis

Further research was performed to define a geometrical configuration that would allow faster/higher pulses. Thus, a hydrogen/air blend was used for this aim to minimise the complexity of the calculation and avoid mixture/turbulence effects still barely understood. Thus, a 2D simulation was performed using Hydrogen/air blends with OpenFOAM [15]. The code uses differential conservation of mass, momentum and energy equations together with the equation of state for ideal gas for compressible flows. According to Godunov's scheme, each contacting cell was considered to be a Riemann problem. Godunov's scheme [16] is a conservative method that has been used to calculate the convective flow at the cell surface without using the time expensive iterative scheme.

A stoichiometric hydrogen/air mixture was used in a 21.2mm internal diameter and 1500mm length tube. Ignition starts at the left end of the tube, and the right end was open to the atmosphere. As shown in Figure 2, three types of obstacles (rectangular, semi-circular and triangular cross-sections) were used to increase the flame turbulence, which decreases the transition-to-detonation distance. The blockage ratio for the three configurations was kept constant at 47%.



Figure 2. Obstacles shapes.

## Results and Discussion

### Natural Gas/Oxygen Mixture Results

The three composition of shale gas proposed by Stamford and Azapagic [10] were mixed with pure oxygen over equivalence ratios between 0.2-4.0 and used as reactants. The product pressure, velocity and temperature are drawn with respect to the volume ratio, that is fuel volume to the total mixture volume. Also, the reactants mole fractions calculated by GASEQ were used in CHEMKIN-PRO as input in conjunction with the shock velocity calculated using the pressure of the shock from, using equation (1),

$$u_s = c_s \sqrt{\frac{\gamma+1}{2\gamma} \left( \frac{p_2}{p_1} - 1 \right) + 1} \quad (1)$$

The velocity obtained in CHEMKIN was used to calculate the velocity induced by the shock using equation (2)

$$u = \frac{2c_s}{\gamma+1} \left( M_s - \frac{1}{M_s} \right) \quad (2)$$

where,  $u_s$  is shock velocity,  $c_s$  is speed of sound in shock conditions,  $\gamma$  is specific heat ratio,  $p_2$  and  $p_1$  are the pressure before and after the shock respectively,  $u$  is the induced velocity, and finally  $M_s$  is the shock Mach number.

Both simulations show similar behaviour for pressure, velocity and temperature produced by the detonation for the three cases of shale gas composition. Although the dilution of fuel-oxygen mixtures reduces thermal energy, it changes the mixture heat capacity and as a result it increases combustion temperature. The molecular mass of the diluent has a significant effect on DDT time. For example, helium dilution causes the detonation velocity to increase and therefore decrease the DDT time due to its low molecular weight, whilst carbon dioxide and nitrogen increase DDT time and significantly inhibit deflagration to detonation processes [17].

The pressure of the products calculated using GASEQ and CHEMKIN are shown in Figure 3. It was found that the pressure for the three cases is almost the same, with slightly higher values for those calculated by CHEMKIN. The maximum pressure was achieved at a fuel volume fraction of around 40% of the total oxy-fuel mixture. The higher pressure was found to be reached using the third case composition, which is mainly due to higher concentration of hydrocarbons in the blend, despite the lower concentration of methane.

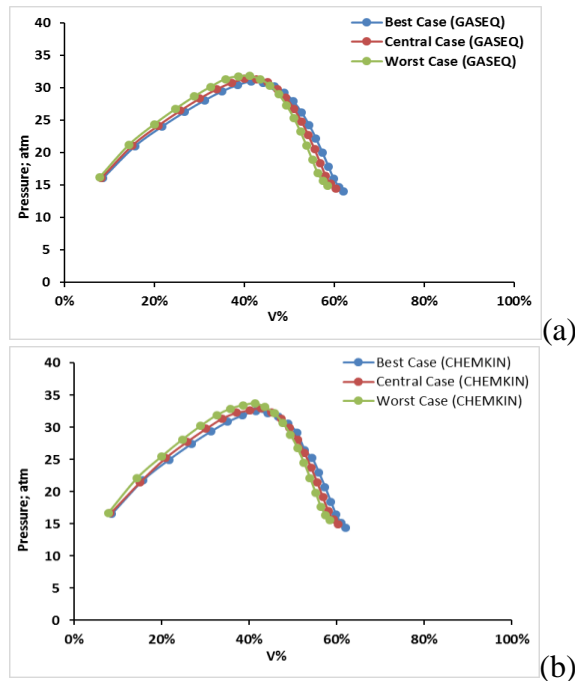


Figure 3. Products pressure versus fuel volume % for hydrocarbon/oxygen mixture,

a) GASEQ; b) CHEMKIN-PRO.

Figure 4 shows the velocity profiles of the products calculated by GASEQ and CHEMKIN. Although the trends of velocity behave in the same manner as those of pressure in figure 3, the maximum values of velocity are shifted further to the rich side of the mixture. The main factor responsible for this shift is products dissociation. Furthermore, the increase of the total low molecular mass species in the products, as shown in Figure 5, leads to the increase of velocity until a point where the total molecular mass of these species starts decreasing with the increase of denser species.

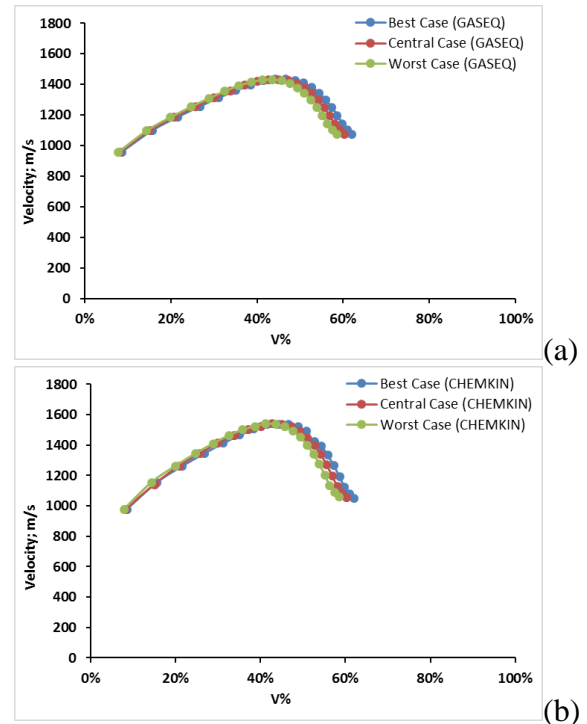


Figure 4. Products velocity versus fuel volume % for hydrocarbon/oxygen mixture, a) GASEQ; b) CHEMKIN-PRO.

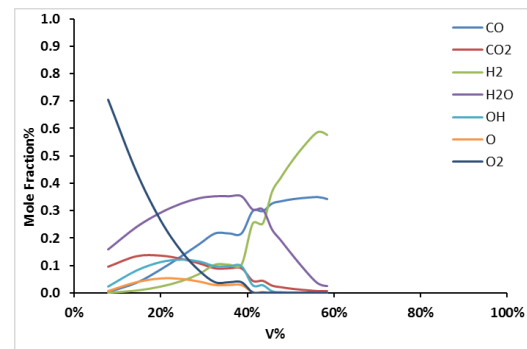


Figure 5. Primary product species versus fuel volume % for hydrocarbon/oxygen mixture.

### Hydrogen/Air Mixture Results

In order to compare the validity of the CFD calculations, hydrogen/air mixtures were used to

calculate thermodynamic parameters. Again, the calculations were undertaken over equivalence ratios between 0.2 to 4.0.

The results for products pressure using both codes are very similar. The maximum pressure was attained slightly rich of the stoichiometric conditions. This is related mainly to the corresponding laminar flame speed. The products velocity showed continuous increase in both simulations, with indiscernible differences for volume fractions between 19% and 44%. The more detailed CHEMKIN-PRO reaction mechanisms will influence the reaction rates including reactants and products concentration, which in turn affect products heat capacity and the results of equation (2). The increase in the velocity of products for hydrogen/air mixtures is due to the continuous increase in hydrogen content beside the change in the energy content, see Figure 7.

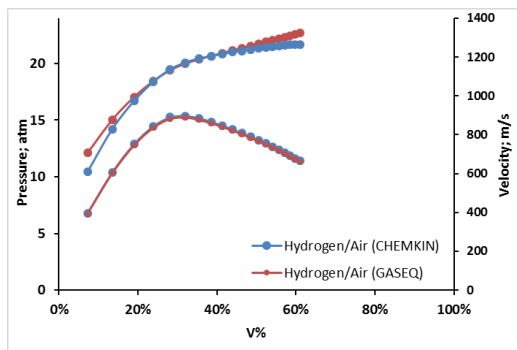


Figure 6. Products pressure and velocity versus hydrogen volume % for hydrogen/air mixture a) GASEQ; b) CHEMKIN-PRO.

Unlike the hydrocarbon/oxygen mixture, the products over-pressure for hydrogen/air mixture reduces less steeply on the rich side compared to the lean side of the peak value. This is attributed to the apportionment of high hydrogen concentration in the products.

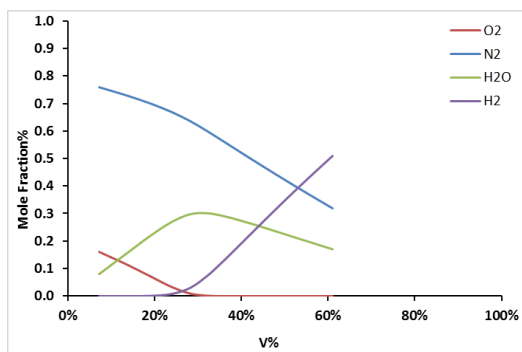


Figure 7. The most dominant product species versus hydrogen volume % for hydrogen/air mixture.

Although the pressure produced from hydrocarbon/oxygen mixture is almost about twice the pressure produced from hydrogen/air mixture, and the velocity produced from the former is 1.2 times the velocity produced from the latter, both

mixtures show similar behaviour over the region bounded by the flammability limits.

The detonation velocity for both mixtures was calculated using GASEQ software, Figure 8. Using pure oxygen increased the detonation velocity for hydrocarbons over that for hydrogen/air. Results illustrate similar behaviour for both mixtures until the velocity reaches a turning point for hydrocarbons.

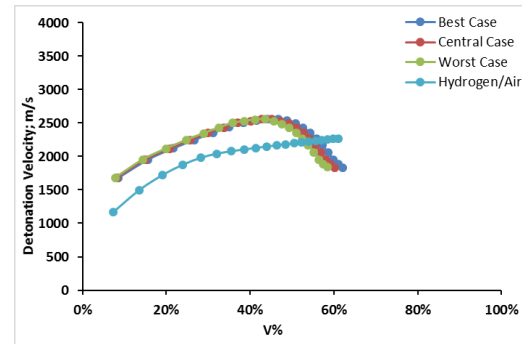


Figure 8. Detonation velocity versus fuel volume % for hydrocarbon/oxygen and hydrogen/air mixtures, GASEQ.

## CFD Results

A 2-dimensional simulation was used to differentiate the relative performance between various internal geometries to find the most effective in producing higher over-pressure and shorter transition distance. Three geometries are discussed in this paper, namely rectangular, semicircular and triangular designs. The domain is divided into ten equal parts along the x-axis, each part being 150mm long measured from centre-to-centre spacing between obstacles. Each obstacle was 10mm long.

The flame velocity, pressure and temperature results are presented in Figure 9. The internal geometry of the detonation tube influenced the combustion propagation significantly. The time required to consume the reactants was less for the tube with rectangular and triangular obstacles than for the tube fitted with semicircular obstacles. This has been ascribed to the sharp edges in the cross-section of the first two geometries, which increases drag and its influence on the degree of induced recirculation.

The simulation results also showed that flame speed exceeded the detonation speed threshold in the tube with rectangular obstacles at  $t=6.95\text{ms}$ , when the flame passes the seventh obstacle. For the semicircular obstacles, detonation speed threshold is exceeded at time  $t=8.25\text{ms}$  by the eighth obstacle of the tube. Finally, the detonation speed threshold is achieved earlier with triangular obstacles, where the flame passes the sixth obstacle at  $t=7.15\text{ms}$ . The results indicate that the flame speed using rectangular obstacles passes through number of conditions that force it to decelerate forming the tulip flame. Moreover, the increase of pressure at the corners of rectangular obstacles increases the Rayleigh-Taylor instability. On the other hand, although the velocity

in the tube with semicircular obstacles is the lowest among the three configurations, the pressure reaches the highest value.

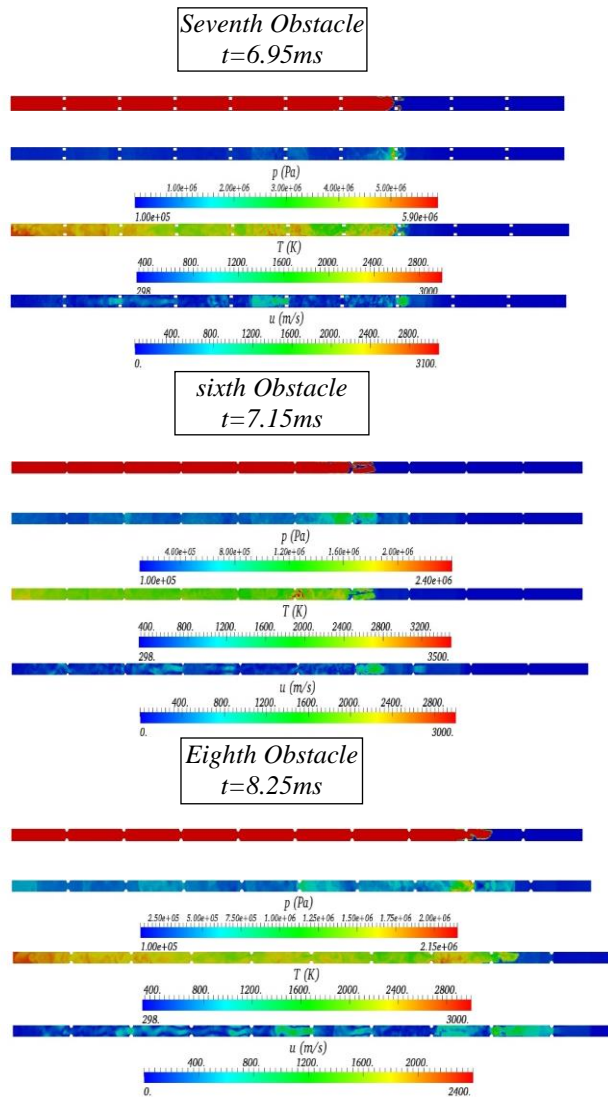


Figure 9. Detonation location and time for three internal geometry configurations.

A phenomenon of importance for all geometries is shock reflection, which has a crucial effect on the pressure and velocity gradient along an obstructed tube. When the shock wave hits the upper surface of an obstacle it reflects, and when it passes the obstacle two more waves are generated: an expansion wave and a reflection wave. While the reflection wave strengthens the incident shock, the expansion wave weakens it. Mach stem (the wave formed by incident and reflected shock waves fusion) will be generated between the high pressure incident-reflected waves and the low pressure incident-expansion waves. The upper side width of the obstacle plays a pivotal role in generating the expansion wave. Wider upper?? side obstacles produce higher Mach stem and higher incident shock pressures as a result. The windward??? slope (for triangular cross-section obstacles) also has considerable influence on the

incident shock strength. For the positive slope of the triangular obstacle, the reflected wave is generated as soon as the incident shock touches the obstacle edge. Thus, there is a phenomenon of more expansion-contraction as a consequence of this early reflected shock, and therefore the higher incident shock pressure [18].

The pressure and velocity gradient along the obstructed tube have been presented with respect to tube length, figure 10, and time, figure 11. The pressure increases considerably when the gas reaches an obstacle. The maximum pressure is attained by the eighth obstacle for the rectangular cross-section geometry obstacles, and by the end of the tube for both semicircular and triangular obstacles. Notwithstanding, the higher pressure rise has been obtained with the tube equipped with semicircular obstacles.

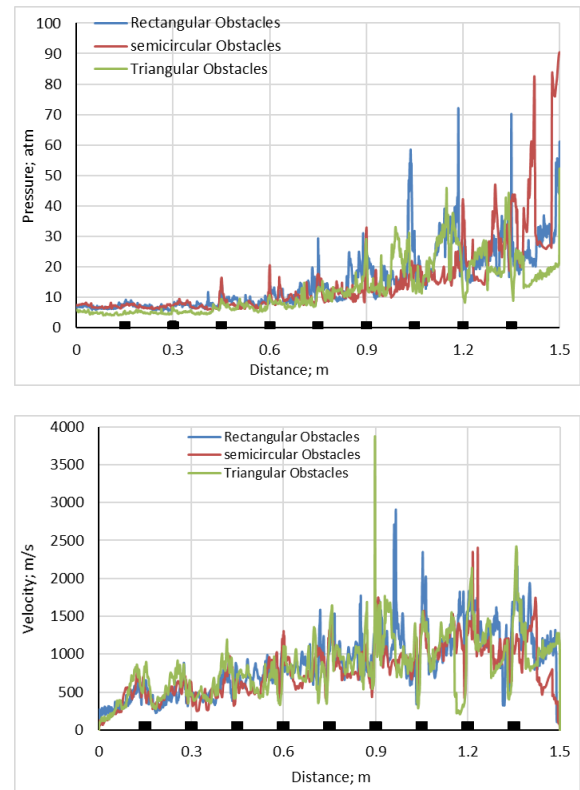


Figure 10: Pressure and velocity for three internal geometry configurations along the tube.

Velocity, on the other hand, demonstrated higher fluctuations along the tube. This was mainly due to the different stages that the flame passes by, which accelerate and decelerate the flame depending on the turbulence and inherent instabilities. As the triangular obstacles provide the highest turbulence in the flow, this profile produced the maximum fluctuations among the three geometries. Furthermore, the detonation velocity threshold is exceeded at shorter distances, with the triangular obstacle.

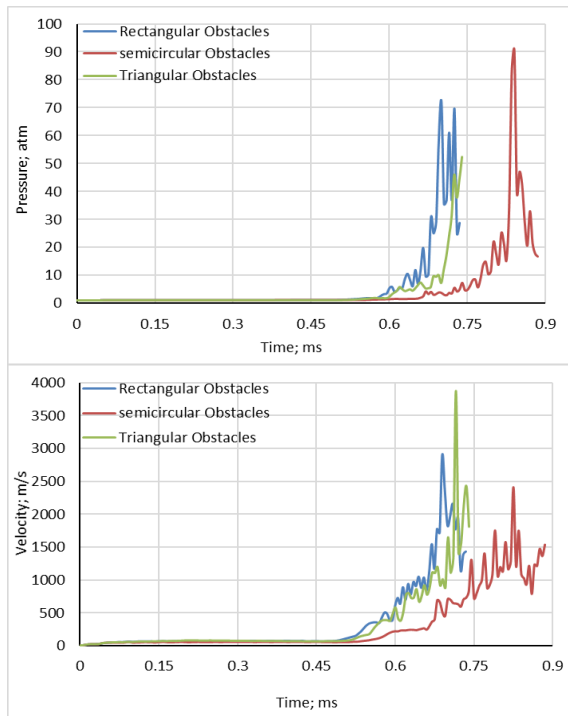


Figure 11. Pressure and velocity for three internal geometry configurations along the tube with respect to time of combustion progress.

## Conclusions

Detonation products, pressure and temperature have been numerically analysed using three software with different shale gas and hydrogen/air blends. For shale gas, it was found that the maximum pressure and velocity were achieved with a fuel volume fraction that exceeds 40% of the total hydrocarbon/oxygen mixture, with He increasing the propensity of detonation while inert reduce transition from deflagration.

Studies with hydrogen allow the study of three different internal geometries using CFD with OpenFOAM. The maximum pressure was achieved with semicircular cross-section obstacles, reaching pressures ~90atm. However, the deflagration to detonation transition distance was found to be shorter in the tube equipped with triangular obstacles. Further research and experimental correlation is sought using all these blends and obstacles.

## References

- [1] P. Stevens, "The 'Shale Gas Revolution': Hype and Reality," 2010.
- [2] L. Gandossi, "An overview of hydraulic fracturing and other formation stimulation technologies for shale gas production," 2013.
- [3] Society of Petroleum Engineers, "Fracturing fluids and additives," PetroWiki. SPE International, 2014.
- [4] S. S. Suthersan, Remediation Engineering: Design concepts. 1997.
- [5] A. Rogala, K. Książniak, and J. Hupka, "Perforating systems in shale gas recovery," PhD Interdiscip. J., 2013.
- [6] S. Kerampran, D. Desbordes, and B. Veyssière, "Propagation of a flame from the closed end of a smooth horizontal tube of variable length," in Proceedings of the 18th ICDERS, 2001.
- [7] C. CLANET and G. Searby, "On the 'Tulip Flame' Phenomenon," Combust. Flame, vol. 105, no. 1–2, pp. 225–238, 1996.
- [8] Porowski, R. and Teodorczyk, a. 2013. Experimental study on DDT for hydrogen–methane–air mixtures in tube with obstacles. Journal of Loss Prevention in the Process Industries 26(2), pp. 374–379.
- [9] W. Breitung, C. Chan, S. Dorofeev, A. Eder, B. Gelfand, M. Heitsch, R. Klein, A. Malliakos, E. Shepherd, E. Studer, and P. Thibault, "Flame Acceleration and Deflagration-to-Detonation Transition in Nuclear Safety," 2000.
- [10] L. Stamford and A. Azapagic, "Life cycle environmental impacts of UK shale gas," Appl. Energy, vol. 134, pp. 506–518, Dec. 2014.
- [11] C. Morley. (2005, 30/10/2012). Gaseq Chemical Equilibrium Program. Available: <http://www.gaseq.co.uk>
- [12] Reaction-Design (May 2013), [Online]. Available: <http://www.reactiondesign.com>
- [13] Reaction-Design (October 2012), Fuel Models for Accurate Simulation. Available:<http://www.reactiondesign.com>.
- [14] Gregory P. Smith, David M. Golden, Michael Frenklach, Nigel W. Moriarty, Boris Eiteneer, Mikhail Goldenberg, C. Thomas Bowman, Ronald K. Hanson, Soonho Song, William C. Gardiner, Jr., Vitali V. Lissianski, and Zhiwei Qin [http://www.me.berkeley.edu/gri\\_mech/](http://www.me.berkeley.edu/gri_mech/)
- [15] F. Ettner: Efficient numerical simulation of the deflagration to detonation transition. Ph.D. Thesis (in German), Technical University of München, 2013.
- [16] Godunov's scheme. Available on line: [https://en.wikipedia.org/wiki/Godunov%27s\\_scheme](https://en.wikipedia.org/wiki/Godunov%27s_scheme)
- [17] E. Schultz, E. Wintenberger, and J. Shepherd, "Investigation of Deflagration to Detonation Transition for Application to Pulse Detonation Engine Ignition Systems," Proc. 16th JANNAF Propuls. Symp., vol. 1, no. c, pp. 175–202, 1999.
- [18] S. Sha, Z. Chen, and X. Jiang, "Influences of obstacle geometries on shock wave attenuation," Shock Waves, vol. 24, no. 6, pp. 573–582, Nov. 2014.